

Experimental Study of the Contact Forces and Deformations of Mortise-and-Tenon Joints Considering the Fits and Grain Orientations of the Tenon

Wengang Hu,^{a,b} Na Liu,^b and Huiyuan Guan^{a,b}*

A method to measure the contact forces and deformations of mortise and tenon joints based on previous theoretical studies was proposed. The influence of the tenon fits and grain orientations on the contact forces and deformations of the mortises and tenons were studied using this method. The testing method and equations were all introduced in detail. The results showed that the contact force between the mortise and tenon with the tenon in the radial grain orientation was larger than that for the tenon in the tangential grain orientation with the same tenon fit. An exponential relationship between the contact force and tenon fit was found. Also, the deformation of the mortise was 3.6 times smaller than the tenon with a tangential grain orientation and 2.2 times smaller than the tenon with a radial grain orientation.

Keywords: Mortise-and-tenon; Furniture joints; Contact force; Deformation

Contact information: a: Co-Innovation Center of Efficient Processing and Utilization of Forest Resources, Nanjing Forestry University, 210037 Nanjing, China; b: Department of Furniture Design, Nanjing Forestry University, 210037 Nanjing, China;

** Corresponding author: hwg@njfu.edu.cn*

INTRODUCTION

Mortise-and-tenon joint furniture has a long history. It is popular because it combines functional, technical, and artistic aspects. The strength of this furniture does not rely on the member itself, but on the joint (Eckelman 1971; Li *et al.* 2014; Smardzewski *et al.* 2014; Hu *et al.* 2017; Hu *et al.* 2018). In recent years, many studies on the factors that influence the strength of mortises and tenons, such as the interference fit (Zhong and Guan 2007), tree species and glue types (Smardzewski 2002; Ratnasingam and Ioras 2013; Záborský *et al.* 2017), and tenon shape and geometry (Sparkes 1968; Hill and Eckelman 1973; Erdil *et al.* 2005; Tankut and Tankut 2005; Kasal *et al.* 2016), have been performed with T- and L-shaped specimens. However, the contact forces and deformations of mortises and tenons have not been studied thoroughly by experimental methods.

It is known that the contact forces and deformations of mortises and tenons depend on the tenon fit and play an important role in mortise-and-tenon furniture structure design. The withdrawal load resistance of mortise-and-tenon joint is determined by the contact force and friction coefficient between the mortise and tenon. Previous studies have reported that the withdrawal load resistance and bending load resistance are proportional to the tenon fit (Tankut and Tankut 2005; Zhong and Guan 2007; Kasal *et al.* 2016). Hu and Guan (2017a) set up a mathematical model for predicting the contact force between mortises and tenons in an elastic range of wood by simplifying the mortise-and-tenon joint to a two-dimensional structure. Diler *et al.* (2017) investigated

the withdrawal force capacity of T-type furniture joints constructed from various heat-treated wood species. The results showed that the heat treatment reduced the withdrawal force capacity of joints by 25% compared with joints constructed from control specimens. This was because the heat treatment decreased the contact force between the mortise and tenon. Although there are few studies on the contact forces and deformations of mortises and tenons, with the development of computer technology and the finite element method (FEM), many studies have tried to analyze the stress and strain distributions of mortise and tenon joints. Smardzewski and Papuga (2004) studied the stress distributions in angle joints of skeleton furniture with the FEM. Wang and Lee (2014) investigated the design feasibility and analyzed the interference fit in dowel-glued joints with the FEM. Derikvand and Ebrahimi (2014) studied the stress and strain distributions of T-shaped mortise and loose tenon furniture joints under uniaxial bending loads with the FEM. The stress and strain distributions in joints were estimated by ANSYS finite element software. The results indicated that the shear stress and shear elastic strain values in joint elements generally increased with the tenon dimensions and corresponding bending moment capacities. Although the FEM and mathematical model can be applied to study the contact forces and deformations of mortise and tenon joints, the accuracy was not ensured because no experimental tests were performed to validate it.

The aim of this study was to provide an experimental method of testing the contact forces and deformations of mortises and tenons. The effects of the tenon fits and grain orientations on the contact forces and deformations of mortises and tenons were studied. This method will help to further understand the strength of mortise-and-tenon joint furniture.

EXPERIMENTAL

Materials

The material used in this study was beech (*Fagus orientalis* Lipsky), which was bought from a local wood commercial supplier (Nanjing, China). The average density was 0.63 g/cm³, and the moisture content was conditioned to and held at 11.2% before and during the experiment. The width of the annual ring was approximately 1.3 mm, and the ratio of early wood to late wood was nearly 1:3. In addition, according to the previous testing results (Hu and Guan 2017b), the elastic moduli and yield strengths of beech in the longitudinal (L), radial (R), and tangential (T) grain orientations are as shown in Table 1.

Table 1. Mechanical Properties of Beech Wood

Mechanical properties	Grain orientations		
	L	R	T
Elastic moduli (MPa)	12205	1858	774
Yield strength (MPa)	42.51	9.83	4.49

Description of the Specimens

All of the specimens used in this study were processed using a computer numerical control (CNC) machine with an accuracy of 0.01 mm (WPC, Shanghai, China). Firstly, the mortises and tenons were machined to the following dimensions: 30 mm (depth) × 30 mm (length) × 16 mm (width) for the mortise, and 30 mm (length) × 30

mm (height) \times 15.8 mm (thickness) for the tenon. The tenon fit between mortise and tenon were chosen according to processing technology of real mortise-and-tenon joint, *i.e.*, the mortise width and tenon thickness are clearance fit, and the mortise height and tenon width are interference fit, as shown in Fig. 1. The tenon fit refers to the interference fit between mortise height and tenon width.

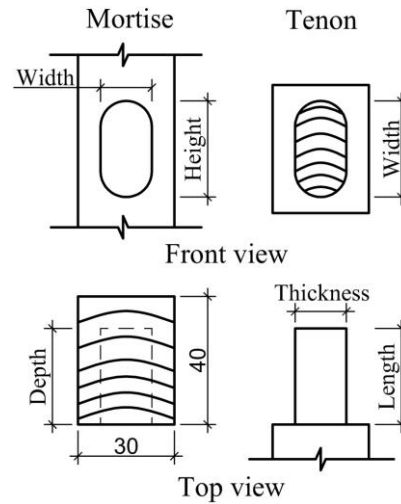


Fig. 1. Definition of tenon fit between mortise and tenon

Secondly, the mortises were divided into two equal parts by an arm saw with a 4-mm-thick blade, and then all of the burrs on the specimens were carefully sanded with sandpaper to ensure that the mortise and tenon could be assembled seamlessly. The dimensions of the specimen are shown in Fig. 2, and the grain orientations in the width direction of the tenon were categorized in the radial and tangential directions. Figure 2a only shows the tenon width in the radial direction, and the tangential direction was perpendicular to it. In the loading direction, the mortise was in the longitudinal grain orientation.

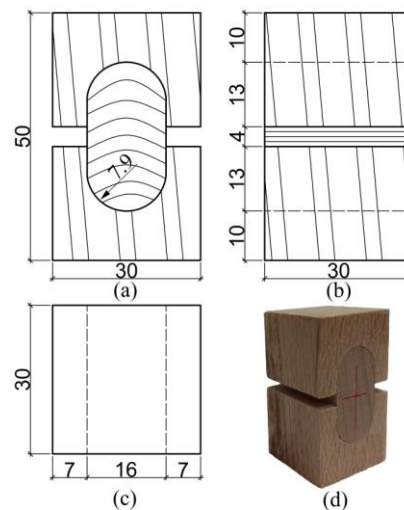


Fig. 2. Dimensions (mm) of the specimen: (a) front view, (b) left view, and (c) top view; and (d) photo of the specimen

Testing Methods

This method was put forward based on the thought of approximate equivalence. The contact force between mortise and tenon results from the interference fit. It is difficult to measure the contact force between mortise and tenon in the assembled state, so the method in this paper was put forward. The displacement load applied by universal test machine was used to simulate the interference fit between mortise-and-tenon joint. It follows that the load outputted by testing machine is the contact force between the mortise and tenon joint.

The equipment used in this study was a 20-kN universal testing machine (AGS-X, Shimadzu, Kyoto, Japan) with a steel mold designed by the authors, which is shown in Fig. 3. The loading speed was 0.5 mm/min, which was controlled by displacement methods, and a 10-N preload was imposed on the top of the mortise before testing to bring the mortise and tenon into close contact. Then, the universal testing machine was loaded until it reached the specified displacement. In this paper, the displacement was set to 0.1 mm, 0.2 mm, 0.3 mm, 0.4 mm, and 0.5 mm, which corresponded to different tenon fits between the mortise and tenon.

Figure 3a shows the method of measuring the contact force between the mortise and tenon. The wood specimen was placed in the steel mold, and then the testing machine began loading according to the method described above. To determine the deformations and stiffness of the mortise and tenon, additional tests had to be conducted. Figure 3b shows the method used to determine the stiffness of the tenon, where the wood mortise was replaced by a steel mortise. The loading method was the same as described above, and then the stiffness of the tenon was calculated with Eq. 1 for the linear stage of the load-displacement curve. Figure 3c shows the method of determining the stiffness of the mortise by the same loading method, but the wood tenon was replaced by a steel tenon. The stiffness of the mortise was calculated with Eq. 1 for the linear stage of the load-displacement curve:

$$K = \Delta F / \Delta U \quad (1)$$

where K is the stiffness (N/mm), ΔF is the change in the load in the linear stage of the load-displacement curve (N), and ΔU is the change in the deformation (mm).

In total, 200 measurements were repeated for five tenon fits and two grain orientations. In addition, the influences of the tenon fits and grain orientations on the contact forces and deformations were determined with an analysis of variance (ANOVA) and Fisher's F-test with SPSS 22 software (Nanjing, China).

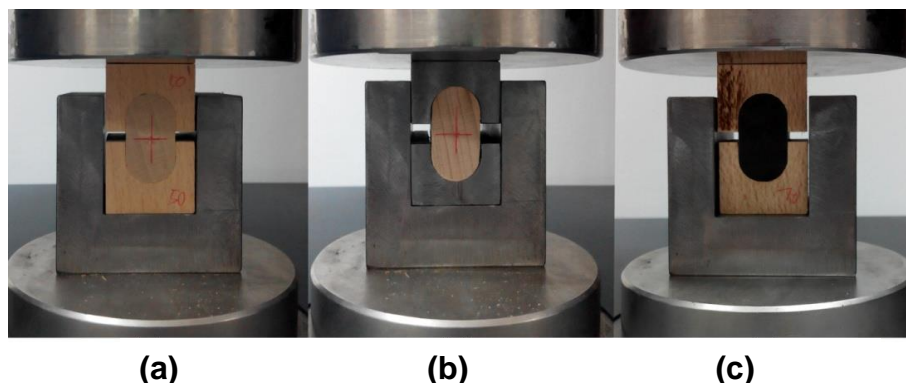


Fig. 3. Setup for measuring the (a) contact forces of the mortises and tenons, (b) stiffness of the tenon, and (c) stiffness of the mortise

RESULTS AND DISCUSSION

Contact Force between the Mortise and Tenon

Figure 4 shows the results of the contact forces between the mortise and tenon with different tenon fits in the radial and tangential grain orientations, according to the method that is shown in Fig. 3a. The correlations between the contact forces and tenon fits in the radial and tangential grain orientations were fitted, as shown by Eqs. 2 and 3, respectively, which suggested an exponential relationship between the contact force and tenon fit:

$$F_t = -589 + 510e^{x/0.375} \quad R_t^2 = 0.99867 \quad (x \geq 0.1) \quad (2)$$

$$F_r = -525 + 444e^{x/0.297} \quad R_r^2 = 0.99884 \quad (x \geq 0.1) \quad (3)$$

where F_t and F_r are the contact forces between the mortises and tenons in the tangential and radial grain orientations (N), respectively, x is the tenon fit (mm), and R_t^2 and R_r^2 are the correlation coefficients of Eqs. 2 and 3, respectively.

Their coefficients of determination were all above 0.99. Furthermore, the contact force for the tenons with a radial grain orientation was larger than that for the tenons with a tangential grain orientation in the same tenon fit. This can be explained by the mechanical properties of beech wood shown in Table 1. It is apparent from the table that the elastic moduli and yield strength in radial grain orientation were all larger than those in tangential grain orientation.

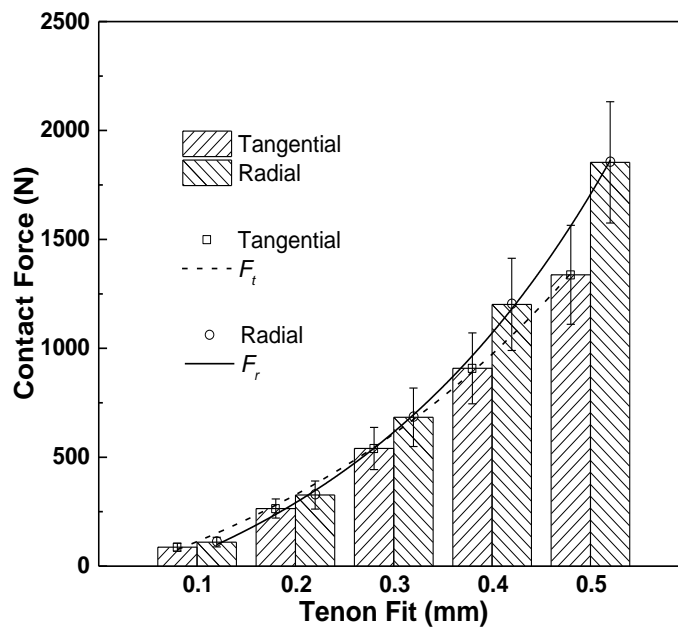


Fig. 4. Contact forces between the mortises and tenons with different tenon fits and grain orientations

Stiffness of the Mortise and Tenon

Figure 5 shows the contact forces between the mortises and tenons in the radial and tangential grain orientations with different tenon fits, according to the method that is shown in Fig. 2b. Their contact forces were linearly fitted, as shown by Eqs. 4 and 5:

$$F_{T-t} = 3496.5x - 289 \quad R_{T-t}^2 = 0.99349 \quad (x \geq 0.1) \quad (4)$$

$$F_{T-r} = 5779.8x - 520 \quad R_{T-r}^2 = 0.99183 \quad (x \geq 0.1) \quad (5)$$

where F_{T-t} and F_{T-r} are the contact forces of the tenons in the tangential and radial grain orientations (N), respectively, x is the tenon fit (mm), and R_{T-t}^2 and R_{T-r}^2 are the correlation coefficients of Eqs. 4 and 5, respectively.

The coefficients of determination again were all above 0.99, which suggested that the load-displacement curves with the tenons in the tangential and radial grain orientations were all in the linear stage. Therefore, the slopes of Eqs. 4 and 5 were the stiffness of the tenons in the radial and tangential grain orientations, respectively. As a result, the stiffness of the tenons with a radial grain orientation (K_{T-r}) was 5779.8 N/mm and that of the tenons with a tangential grain orientation (K_{T-t}) was 3496.5 N/mm. These equations also indicated that the contact force between the mortises and tenons with a radial grain orientation was larger than that of the tenons with a tangential grain orientation. In addition, the mechanical properties of beech determined according to standard compressive method was studied by Hu (2017b). The stiffness of beech in radial and tangential grain orientations were 11881 (4.74) and 6878 (4.58) N/mm respectively, which are all larger than those measured in the case of oval tenon specimens. It is known that the size of specimen influence the mechanical properties of wood; similarly, the geometry of sample may also impact stiffness and other mechanical properties of wood. Carpinteri and Pugno (2005) proposed an argument about whether scaling laws on the strength of solids is related to mechanics or to geometry. They proposed that geometry could hold an unexpected and fundamental role.

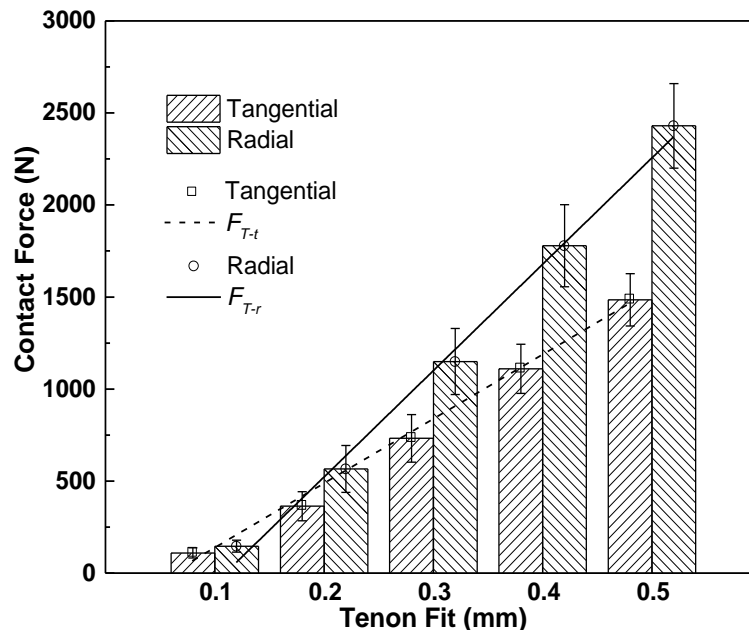


Fig. 5. Contact forces between the mortises and tenons with a steel-made mortise in different tenon fits and grain orientations

Figure 6 shows that the contact forces of the mortises and tenons increased with different tenon fits, according to the method that is shown in Fig. 2c. The relationship between them was linearly fitted, as shown by Eq. 6, and the slope of the fitting line was the stiffness of the mortise:

$$F_M = 12617.1x - 1142 \quad R_M^2 = 0.97595 \quad (x \geq 0.1) \quad (6)$$

where F_M is the contact force of the mortise (N), x is the interference fit (mm), and R_M^2 is the correlation coefficient of Eq. 6.

It was found that the stiffness of the mortise (K_M) was 12617.1 N/mm, which was larger than that of the tenons with radial and tangential grain orientations. This was because the compressed direction of the mortise had a longitudinal grain orientation to the wood and that of the tenon had a radial or tangential grain orientation. It is known that the compression strength of longitudinally oriented wood is greater than in the radial and tangential grain orientations, according to the wood mechanical properties (Hu and Guan 2017b).

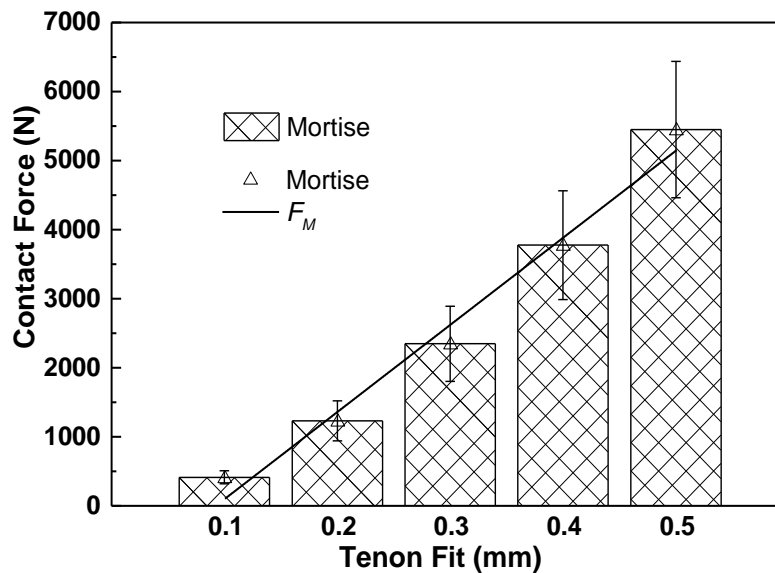


Fig. 6. Contact forces between the mortises and tenons with a steel-made tenon and different tenon fits

Deformation of the Mortise and Tenon

The stiffness values of the mortises and tenons in different grain orientations were obtained from the above experiments. Then, the deformations of the mortises and tenons were calculated according to Eqs. 7 and 8.

$$F = K_T x_1 = K_M x_2 \quad (7)$$

$$x = x_1 + x_2 \quad (8)$$

where F is the contact force between the mortise and tenon (N), K_T is the stiffness of the tenon (N/mm), K_M is the stiffness of the mortise (N/mm), x is the tenon fit (mm), x_1 is the deformation of the tenon (mm), and x_2 is the deformation of the mortise (mm).

Figures 7 and 8 show the deformations of the mortises and tenons with different tenon fits and grain orientations, respectively. The deformation of the mortise was smaller than that of the tenon with the same tenon fit and grain orientation, and the

relationship between them was shown by Eq. 7. In this study, the deformation of the mortises was 3.6 times smaller than those of the tenons with a tangential grain orientation and 2.2 times smaller than those with a radial grain orientation because the stiffness of the wood in the longitudinal grain orientation was larger than in the radial and tangential grain orientations.

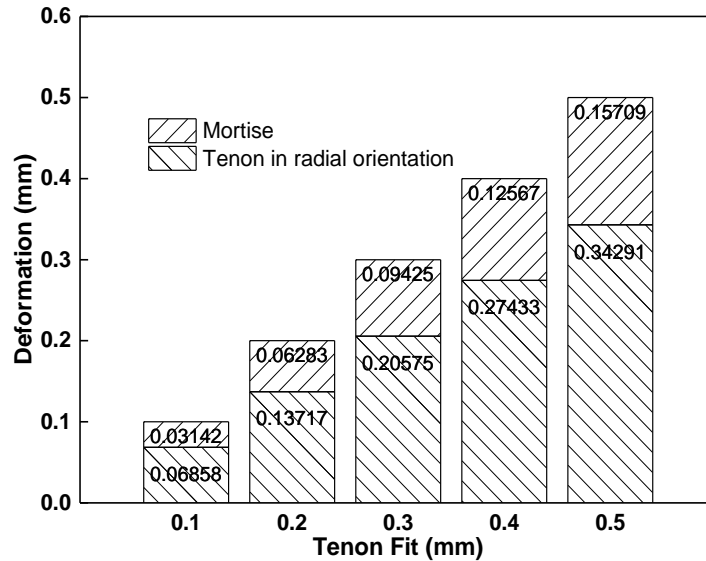


Fig. 7. Deformations of the mortise and tenon with a radial grain orientation and different tenon fits

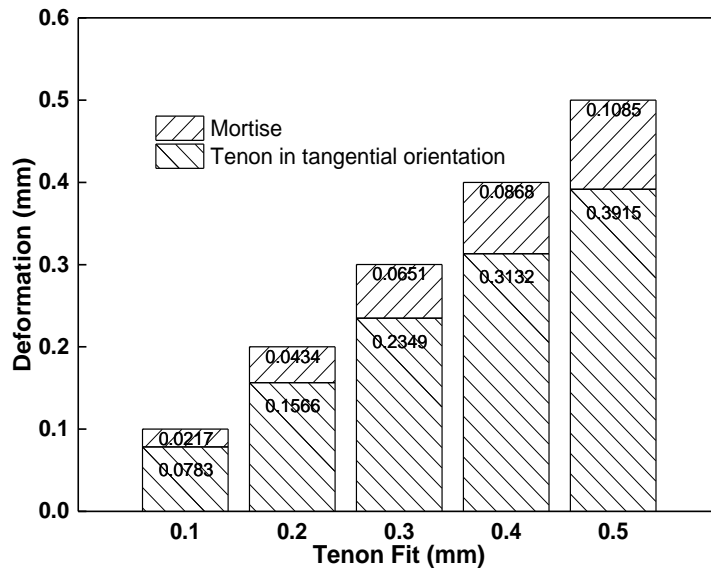


Fig. 8. Deformations of the mortise and tenon with a tangential grain orientation and different tenon fits

The result of ANOVA showed that the tenon fits, grain orientations, and their interaction were all considered to be statistically significant with a *p*-value less than 0.01. Through this method, the contact forces and deformations of the mortises and tenons were able to be measured.

CONCLUSIONS

The contact forces and deformations of the mortises and tenons with different tenon fits were studied by a new method proposed in this paper. The following conclusions were drawn:

1. There was an exponential relationship between the contact force and tenon fit. The contact force between the mortises and tenons with a radial grain orientation for the tenon was larger than with a tangential grain orientation.
2. The stiffness of the mortises was larger than that of the tenons in the radial and tangential grain orientations because the compressed direction of the mortise was in the longitudinal grain orientation.
3. The deformation of the mortises was 3.6 times smaller than that of the tenons with a tangential grain orientation and 2.2 times smaller those with a radial grain orientation.
4. It was concluded that the testing method proposed in this paper can be applied to determine the contact forces and deformations between mortises and tenons. Further studies should focus on the relationship between the strength of mortise-and-tenon joints, and the contact forces and deformations of mortises and tenons based on this method. This will help to further understand the factors that influence the strength of mortise-and-tenon joint furniture.

ACKNOWLEDGMENTS

This study was supported by Scientific Research Foundation of Nanjing Forestry University (GXL2019074); A Project Funded by the National First-class Disciplines (PNFD), and A Priority Academic Program Development of Jiangsu Higher Education Institutions (PAPD).

REFERENCES CITED

- Carpinteri, A., and Pugno, N. (2005). "Are scaling laws on strength of solids related to mechanics or to geometry," *Nat. Mat.* 4, 421-423. DOI: 10.1038/nmat1408
- Derikvand, M., and Ebrahimi, G. (2014). "Finite element analysis of stress and strain distributions in mortise and loose tenon furniture joints," *J. Forestry Res.* 25(3), 677-681. DOI: 10.1007/s11676-014-0507-5
- Diler, H., Acar, M., Balıkcı, E., Demirci, S., and Erdil, Y. Z. (2017). "Withdrawal force capacity of T-type furniture joints constructed from various heat-treated wood species," *BioResources* 12(4), 7466-7478. DOI: 10.15376/biores.12.4.7466-7478
- Eckelman, C. A. (1971). "Bending strength and moment-rotation characteristics of two-pin moment-resisting dowel joints," *Forest Prod. J.* 21(3), 35-39.
- Erdil, Y. Z., Kasal, A., and Eckelman, C. A. (2005). "Bending moment capacity of rectangular mortise and tenon furniture joints," *Forest Prod. J.* 55(12), 209-213.
- Hill, M. D., and Eckelman, C. A. (1973). "Flexibility and bending strength of mortise and tenon joints," *Furniture Design and Manufacturing* 45(1), 54-61.
- Hu, H., Yang, J., Wang F. L., Zhang Y. M. (2018). "Mechanical properties of bolted

- joints in prefabricated round bamboo structures,” *Journal of Forestry Engineering* 3(5), 128-135. DOI: 10.13360/j.issn.2096-1359.2018.05.020
- Hu, W. G., Bai, J., and Guan, H. Y. (2017). “Investigation on a method of increasing mortise and tenon joint strength of fast growing wood,” *Journal of Beijing Forestry University* 39(4), 101-107. DOI: 10.13332/j.1000-1522.20160400
- Hu, W. G., and Guan, H. Y. (2017a). “Investigation on withdrawal capacity of mortise and tenon joint based on friction properties,” *Journal of Forestry Engineering* 2(4), 158-162. DOI: 10.13360/j.issn.2096-1359.2017.04.025
- Hu, W. G., and Guan, H. Y. (2017b). “Study on elastic constants of beech in different stress states,” *Journal of Forestry Engineering* 2(6), 31-36. DOI: 10.13360/j.issn.2096-1359.2017.06
- Kasal, A., Smardzewski, J., Kuşkun, T., and Erdil, Y. Z. (2016). “Numerical analyses of various sizes of mortise and tenon furniture joints,” *BioResources* 11(3), 6836-6853. DOI: 10.15376/biores.11.3.6836-6853
- Li, S. X., Liu, W. J., and Sun, D. L. (2014). “Comparative study on corner joints strength of fast-growing *Pinus massoniana* wood furniture,” *Journal of Central South University of Forestry and Technology* 34(2), 122-126.
- Ratnasingam, J., and Ioras, F. (2013). “Effect of adhesive type and glue-line thickness on the fatigue strength of mortise and tenon furniture joints,” *Eur. J. Wood Wood Prod.* 71(6), 819-821. DOI: 10.1007/s00107-013-0724-1
- Smardzewski, J. (2002). “Strength of profile-adhesive joints,” *Wood Sci. Technol.* 36(2), 173-183. DOI: 10.1007/s00226-001-0131-3
- Smardzewski, J., Lewandowski, W., and İmirzi, H. Ö. (2014). “Elasticity modulus of cabinet furniture joints,” *Mater. Design* 60, 260-266. DOI: 10.1016/j.matdes.2014.03.066
- Smardzewski, J., and Papuga, T. (2004). “Stress distribution in angle joints of skeleton furniture,” *Electronic Journal of Polish Agricultural Universities* 7(1).
- Sparkes, A. J. (1968). *The Strength of Mortise and Tenon Joints*, Furniture Industry Research Association, Stevenage, UK.
- Tankut, A. N., and Tankut, N. (2005). “The effects of joint forms (shape) and dimensions on the strengths of mortise and tenon joints,” *Turk. J. Agric. For.* 29(6), 493-498.
- Wang, Y., and Lee, S.-H. (2014). “Design and analysis on interference fit in the hardwood dowel-glued joint by finite element method,” *Procedia Engineer.* 79, 166-172. DOI: 10.1016/j.proeng.2014.06.326
- Záborský, V., Borůvka, V., Kašíčková, V., and Ruman, D. (2017). “Effect of wood species, adhesive type and annual ring directions on the stiffness of rail to leg mortise and tenon furniture joints,” *BioResources* 12(4), 7016-7031. DOI: 10.15376/biores.12.4.7016-7031
- Zhong, S. L., and Guan, H. Y. (2007). “Relationship between optimal value of interference fit and wood density in oval-tenon joint,” *China Forestry Science and Technology* 21(2), 57-59.

Article submitted: January 1, 2019; Peer review completed: March 17, 2019; Revised version received: May 22, 2019; Accepted: May 23, 2019; Published: September 18, 2019.

DOI: 10.15376/biores.14.4.8728-8737